International Conference on Applied Energy 2019
Aug 12-15, 2019, Västerås, Sweden
Paper ID: 768

THEORETICAL STUDY ON THE PYROLYTIC DEHYDROGENATION MECHANISM OF AMMONIA BORANE

Xiao Tan, Libin Shi, Jiawei Yan, Suitao Qi*

Shaanxi Key Laboratory of Chemical Process Intensification, School of Chemical Engineering and Technology, Xi'an Jiaotong University, Xi'an 710049, China

ABSTRACT

Due to the increasing consumption of traditional fossil energy sources and the resulting environmental problems, the need for new energy sources is increasing. Hydrogen is an efficient and clean energy, and developing a suitable hydrogen storage medium is the key to the use of hydrogen energy. Ammonia borane has attracted much attention due to its high hydrogen storage density (19.6 wt %) and room temperature stability. It can be dehydrogenated by hydrolysis and pyrolysis. At present, the pyrolytic dehydrogenation mechanism of ammonia borane is still unclear. In this work, the dehydrogenation of ammonia borane (AB), ammonia borane dimer ($(AB)_2$), and the diaminodiborane (DADB) have been studied based on density functional theory (DFT). The results show that the energy barriers of the first and second steps for AB pyrolytic dehydrogenation are 38.58 kcal/mol and 78.14 kcal/mol. $(AB)_2$ dehydrogenation were generated by forming N-H...H-B bond, the energy barriers for the first step (46.45 kcal/mol) is higher than AB. In addition, the energy barrier (21.67 kcal/mol) of DADB to form N-H...H-B bond dehydrogenation is much smaller than $(AB)_2$. It reveals that DADB is easier to dehydrogenate than AB and $(AB)_2$. The above results would provide theoretical guidance for the pyrolytic dehydrogenation of ammonia borane.

Keywords: ammonia borane, density functional theory (DFT), pyrolysis dehydrogenation, reaction mechanism

1. INTRODUCTION

In recent years, due to the increasing consumption of traditional fossil energy and the resulting environmental problems, the need for new energy is increasing day by day [1]. Hydrogen energy is considered as an efficient and clean energy, whereas, the use of hydrogen energy is restricted by the storage and transportation of hydrogen. The use of renewable energy for power generation is greatly affected by natural conditions, and the total amount of energy is unevenly distributed over time. If the excess electric energy can be converted into hydrogen energy and released when there is a shortage of energy, the reasonable allocation of energy can be achieved. So, the key to solve this problem is to develop a suitable hydrogen storage medium. There are many hydrogen storage media to be studied such as carbon-based materials [2], metal hydrogenates [3], organic hydrogenates [4] and complex hydrogenates [5] have been studied. Among of them, ammonia borane has attracted much attention because of its high hydrogen storage density (19.6 wt%) and room temperature stability. Ammonia borane can be dehydrogenated by hydrolysis and pyrolysis. In hydrolysis dehydrogenation process, noble metal catalyst are needed [6-9] and difficult to recover. In addition, the introduction of water would inevitably decrease the actual hydrogen storage density of whole systems. Although pyrolytic dehydrogenation can directly obtain hydrogen only by heating, there are still disadvantages such as high initial dehydrogenation temperature, slow dehydrogenation rate, impurity gas generation, and poor reversibility. The pyrolytic dehydrogenation performance of ammonia borane is often improved by adding a suitable promoter or replacing H atom in ammonia borane with different metal atoms such as Li, Na, K, Ca, Sr, Al, etc. [10-13]. Shaw and Autrey et al [14]. studied the decomposition mechanism of ammonia borane at 88 ℃ by using in situ solid ^{11}B MAS-NMR. They think there are three steps in the decomposition of ammonia borane. Ammonia borane dimer ($(AB)_2$), and diaminodiborane $[BH_4^-][NH_3BH_2NH_3]$ (DADB) were detected in the reaction. However, the reaction mechanism of the ammonia borane pyrolysis dehydrogenation varies with the reaction conditions and the use of catalyst. The possible dehydrogenation pathways of AB, DADB and $(AB)_2$ and the relevant energy barrier data needs to be calculated. Moreover, the principle of intramolecular and intermolecular dehydrogenation of $(AB)_2$ remains to be further studied. In this work, several possible pyrolysis dehydrogenation reaction paths of ammonia borane (AB), ammonia borane dimer $(AB)_2$ and diaminodiborane (DADB) were creatively established. By calculating and comparing the energy barrier of each possible path in the reaction process, the most likely reaction path are determined. These findings would provide theoretical prediction for exploring the most likely dehydrogenation mechanism of ammonia borane under different conditions.

2. CALCULATION METHOD

The mechanism of the pyrolytic dehydrogenation reaction of ammonia borane NH_3BH_3 was calculated using Gaussian 03. It uses Harris functional to generate initial guesses. This functional is an approximation of the DFT non-iterative, which produces an initial trajectory that is more accurate than before. At the same time, it adds a lot of high-precision energy methods, and Its calculation accuracy can reach 10E-8. Iogann Tolbatov et al [15] used the density functional and Gaussian groups to calculate the core-electron binding energy in amino acids with an energy error of less than 0.9 kcal/mol. In addition, when we calculate the energy barrier of the reaction process, each of molecule structure is optimized. These all provide a strong guarantee for the accuracy of the results.

Based on the optimization of the structure and frequency of reactant, transition state, intermediate and product in the reaction path, the thermodynamic analysis data of all optimized structures such as total energy, enthalpy, Gibbs free energy are obtained. The transition state is searched by the TS, QST2 or QST3 method, and the intrinsic reaction coordinate calculation is performed to verify the rationality of the transition state. In addition, there is no virtual frequency in all stable states and only one virtual frequency in the transition state in all of the frequency calculation. It notes that IS, TS and FS in all figures represent the initial reactants, transition states and products, respectively. At the same, Pink, blue and white ball in the ball-and-stick model denote B, N, H atom in all figures.

3. RESULTS AND DISCUSSION

3.1 Structural parameters, Density of states and HOMO-LUMO energy

By calculating structural parameters, density of states and HOMO-LUMO energy, some information such as bond length, covalent action and molecular stability of the molecule can be obtained, The most stable structure of AB, $(AB)_2$ and DADB optimized under B3LYP, 6-311+G**(d, p) units is shown in Fig. 1.

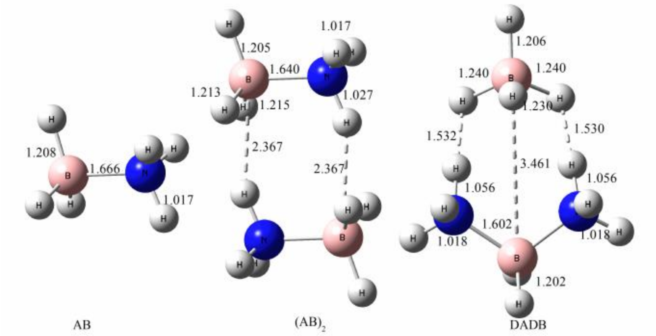

Fig 1 The optimized structure of AB, (AB)2 and DADB (bond length unit: Å)

The total density of states and the density of local states of AB, $(AB)_2$, DADB are calculated. According to the calculation results, DADB has the smallest band gap, AB is the second, and $(AB)_2$ is the largest. It shows that the electronic transition in DADB is easier than $(AB)_2$.

The calculation of HOMO-LUMO energy level difference can be used to measure whether a molecule is easily excited. After calculation, the HOMO-LUMO energy levels of AB, $(AB)_2$, and DADB are 6.56, 7.14, and 6.00 eV, respectively. In summary, under the same conditions, DADB is easier to dehydrogenate than AB and $(AB)_2$.

3.2 Dehydrogenation reaction path of AB

The pyrolytic dehydrogenation of AB is a three-step reaction. Since the third step of dehydrogenation is difficult and the temperature is above 350 °C, the first two steps of dehydrogenation are considered in Figure 2, and the molecular structure and the related bond length are also marked. The potential energy is shown in Figure 3.

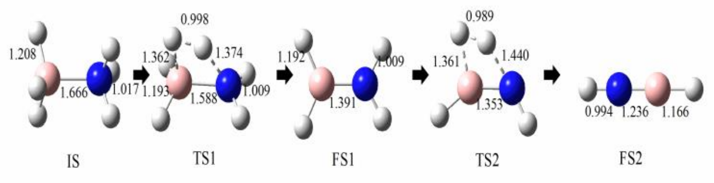

Fig 2 Schematic diagram of the reactants, transition state and product of the AB pyrolytic dehydrogenation reaction process

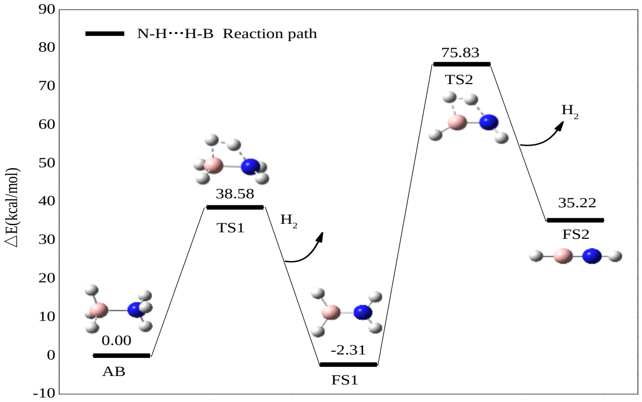

Fig 3 Reaction path of the AB pyrolytic dehydrogenation reaction process

3.3 Dehydrogenation reaction path of $(AB)_2$

The mechanism of intramolecular dehydrogenation of $(AB)_2$ is basically the same as that of AB, and there are two possible paths according to different transition state. The reaction is divided into four steps. First, the initial state IS1 removes one hydrogen molecule to get FS1 via the transition state TS1, and then FS1 changes into FS2-1 or FS2-2 through the transition state TS2-1 or TS2-2. Next, FS3 $(NHBH)(NH_2BH_2)$ is obtained by FS2-1 or FS2-2 via transition states TS3-1 and TS3-2. Finally, FS4 (NHBH)(NHBH) is generated via transition state TS4.

The difference between two paths of $(AB)_2$ dehydrogenation is the second and the third step. The reaction paths and the molecular structure data are shown in Figure 4, and the potential energy is shown in Figure 5.

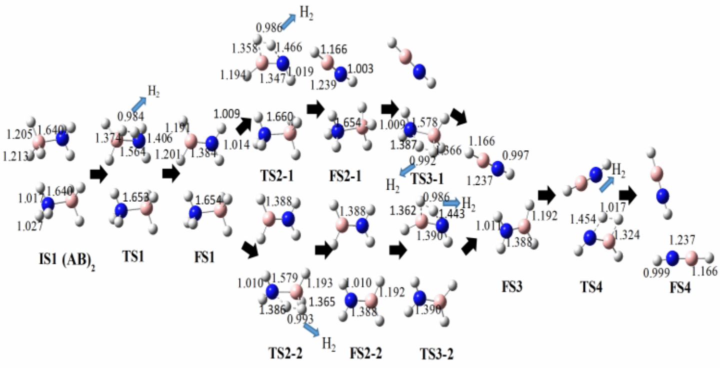

Fig 4 Schematic diagram of the reactants, transition state and product of the $(AB)_2$ pyrolytic dehydrogenation reaction process

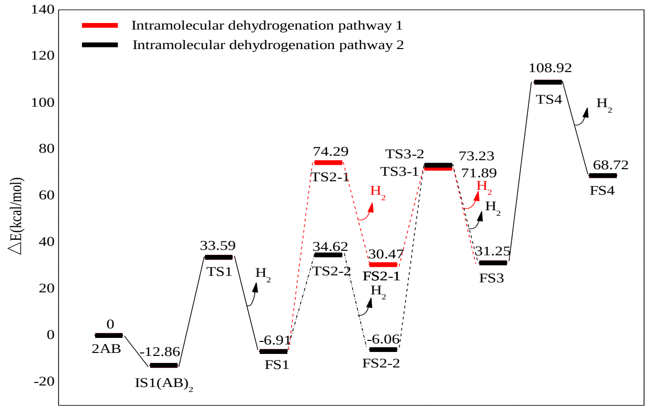

Fig 5 Reaction path of the $(AB)_2$ pyrolysis dehydrogenation reaction process

From the dehydrogenation products of the two dehydrogenation pathways of $(AB)_2$, the second step dehydrogenation products of the two paths are FS2-1 (NHBH)(NH3BH3) and FS2-2 (NH2BH2)(NH2BH2), respectively. The potential energy of the two is 30.47 kcal/mol and -6.06 kcal/mol, respectively, which is lower than the former, indicating that FS2-2 is more stable than FS2-1.

3.4 Dehydrogenation reaction path of DADB

There are two possible pathways for DADB dehydrogenation. In the Path 1, DADB removes one molecule of H_2 via the transition state TSd1 to generate $[BH_4^-][NH_2BHNH_3^+]$ (FSd1). In path 2, DADB removes one molecule of H_2 via transition state TSd2 to form chain-like $NH_3BH_2NH_2BH_3$ (FSd2), and then undergoes isomerization to form $NH_3BH_2NH_2BH_3$ (FSd3) through a transition state TSc. The reaction path and molecular structure are shown in figure 6, the potential energy is shown in Figure 7.

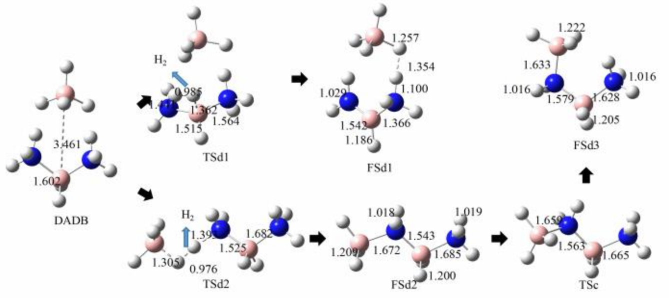

Fig 6 Schematic diagram of the reactants, transition state and product of the DADB pyrolytic dehydrogenation reaction process

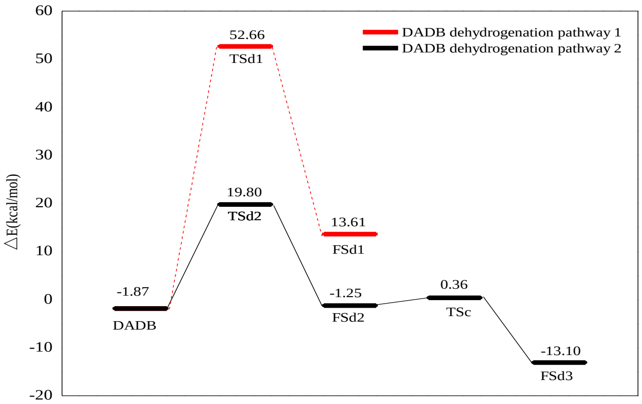

Fig 7 Reaction path of the DADB pyrolytic dehydrogenation reaction process

In the two dehydrogenation paths of DADB, the energy barrier of path 2 (21.67 kcal/mol) is significantly lower than the energy barrier of path 1 (54.53 kcal/mol), indicating that path 2 is more likely to occur. In addition, the energy barrier of the DADB dehydrogenation via path 2 is smaller than that of the AB (38.58 kcal/mol). At the same time, it is also smaller than the energy barrier (46.45 kcal/mol) of the first step of dehydrogenation in the molecule of $(AB)_2$. Therefore, $(AB)_2$ is more likely to be isomerized to form DADB, then DADB is pyrolytic dehydrogenated by path 2c

4. CONCLUSIONS

1) DADB was easier to pyrolytic dehydrogenation than $(AB)_2$ and AB under the same conditions.

2) The energy barriers of the first and the second steps of AB pyrolytic dehydrogenation are 38.58 kcal/mol and 78.14 kcal/mol. And the energy barrier of dehydrogenation in $(AB)_2$ in each step is higher than AB. For AB or $(AB)_2$, the energy barrier for dehydrogenation in the second step is larger than that in the first step, indicating that the second step of dehydrogenation is the control step of the reaction.

3) The energy barrier of dehydrogenation in the first step of DADB via path 2 (21.67 kcal/mol) is smaller than that via path 1 (54.53 kcal/mol), and it is also much smaller than the first step dehydrogenation energy barrier of $(AB)_2$. Hence, DADB is more likely to be dehydrogenated by path 2, and AB may be isomerized to form DADB and then dehydrogenated.

ACKNOWLEDGEMENT

The authors acknowledge the financial support from the Fundamental Research Funds for the Central Universities (No. xjj2016045), China.

REFERENCE

[1] Demirbas A. Potential applications of renewable energy sources, biomass combustion problems in boiler power systems and combustion related environmental issues[J]. Progress in Energy & Combustion Science, 2005, 31(2):171-192.

[3] Strbel R, Garche J, Moseley P T, et al. Hydrogen storage by carbon materials[J]. Journal of Power Sources, 2006,159(2):781

[4] Sakintuna B, Lamari-Darkrim F, Hirscher M. Metal hydride materials for solid hydrogen storage: A review[J]. International Journal of Hydrogen Energy, 2007, 32(9): 1121

[4] Biniwale R B, Rayalu S, Devotta S,et al. Chemical hydrides: A solution to high capacity hy-drogen storage and supply[J]. International Journal of Hydrogen Energy, 2008, 33(1): 360

[5] Orimo S, Nakamori Y, Eliseo J R,et al. Complex hydrides for hydrogen storage[J]. Journal of The American Chemical Society, 2007, 107(10): 4111

[6] Chandra M, Xu Q. A high-performance hydrogen generation system: transition metal-catalyzed dissociation and hydrolysis of ammonia-borane[J]. Journal of Power Sources, 2006, 156(2): 190-194.

[7] Du J, Cheng F, Si M, et al. Nanoporous Ni-based catalysts for hydrogen generation from hydrolysis of ammonia borane[J]. International Journal of Hydrogen Energy, 2013, 38(14): 5768-5774.

[8] Conley B L, Guess D, Williams T J. A robust, air-stable, reusable ruthenium catalyst for dehydrogenation of ammonia borane[J]. Journal of the American Chemical Society, 2011, 133(36): 14212-14215.

[9] Qiu F, Li L, Liu G, et al. Synthesis of Fe0.3Co0.7/rGO nanoparticles as a high performance catalyst for the hydrolytic dehydrogenation of ammonia borane[J]. International Journal of Hydrogen Energy, 2013, 38: 7291-7297.

[10] Xiong Z, Wu G, Chua Y S, et al. Synthesis of sodium amidoborane (NaNH2BH3) for hydrogen production[J]. Energy & Environmental Science, 2008, 1(3): 360-363.

[11] Wu H, Zhou W, Yildirim T. Alkali and alkaline-earth metal amidoboranes: structure, crystal chemistry, and hydrogen storage properties[J]. Journal of the American Chemical Society, 2008, 130(44): 14834-14839.

[12] Luedtke A T, Autrey T. Hydrogen release studies of alkali metal amidoboranes[J]. Inorganic Chemistry, 2010, 49(8): 3905-3910.

[13] Zhang Q, Tang C, Fang C, et al. Synthesis, crystal structure, and thermal decomposition of strontium

amidoborane[J]. The Journal of Physical Chemistry C, 2010, 114(3): 1709-1714.

[14] Stowe A C, Shaw W J, Linehan J C, et al. In situ solid state 11 B MAS-NMR studies of the thermal decomposition of ammonia borane: mechanistic studies of the hydrogen release pathways from a solid state hydrogen storage material[J]. Physical Chemistry Chemical Physics, 2007, 9(15): 1831-1836.

[15] Tolbatov I, Chipman D M, Benchmarking density functionals and Gaussian basis sets for calculation of core-electron binding energies in amino acids[J]. Theoretical Chemistry Accounts, 2017, 136(7).